III SEPOPE

Maio - 18 - 22 / 1992
May - 18 - 22 / 1992

III SIMPÓSIO DE ESPECIALISTAS EM PLANEJAMENTO DA OPERAÇÃO E EXPANSÃO ELÉTRICA

III SYMPOSIUM OF SPECIALISTS IN ELECTRIC OPERATIONAL AND EXPANSION PLANNING

Belo Horizonte (MG) – BRASIL
Belo Horizonte (MG) - BRASIL

THE BRAZILIAN UTILITIES PACKAGE FOR THE ANALYSIS AND CONTROL OF SMALL–SIGNAL STABILITY OF LARGE SCALE AC/DC POWER SYSTEMS

Nelson Martins[1] Leonardo T.G.Lima[2] Herminio J.C.P.Pinto[1] Nilo J.P.Macedo[3]

[1] CEPEL, Caixa Postal 2754, 20.001, Rio de Janeiro, RJ, Brazil
[2] IME, Dept.of Elect. Eng., Praça Gen.Tibúrcio 80, 22.290, Rio de Janeiro, RJ, Brazil
[3] FURNAS Centrais Elétricas S.A., R.Real Grandeza 219, 22.283, Rio de Janeiro, RJ, Brazil

Abstract – The main features of a comprehensive package for the study of small–signal stability problems of very large power systems are presented. This package employs state–of–the–art algorithms for the calculation of dominant eigenvalues, transfer function zeros and residues, participation factors, mode–shapes, time and frequency response plots, synchronizing and damping torques and external system equivalents in the frequency domain. This paper describes the algorithms used in this package, which is denominated PACDYN, and reports results obtained in the study of several test systems.

Keywords – small–signal stability, large scale AC/DC power systems, electromechanical oscillations, sparse eigenanalysis, frequency response techniques, transfer function zeros, transfer function residues, long distance AC transmission, stabilizing signals, static VAr compensators, centralized control, control system design.

I. INTRODUCTION

In the last three decades many instances of unstable oscillations, involving inter–area modes of large power systems, have been observed in various parts of the world. A reliable computer simulation of these modes, regarding both damping and frequency, requires an extensive and detailed representation of the large interconnected system [1].

The development of powerful eigenvalue programs for small–signal stability analysis has been, for some time, recommended by CIGRÉ [2]. Brazilian utilities have been using multimachine eigenvalue programs for the last decade. Many technical reports from individual utilities and multi–utility coordinating councils [3,4,5,6] have been produced based on eigenvalue results. These results were mainly obtained through use of AUTOVAL, a conventional state matrix based multimachine eigenvalue program, developed by CEPEL [7].

AUTOVAL did not completely fulfill the requirements of the Brazilian utilities for a small–signal stability package. In response to their needs, CEPEL has been working for a decade in the development of a state–of–the–art package denominated PACDYN [8,9,10,11,12,13]. A beta version is already available and undergoing tests conducted by FURNAS Electricity Company personnel [14].

Section 2 of this paper contains a brief review of the algorithms employed in the linear analysis of the small–signal electromechanical stability of large power systems.

The major characteristics of PACDYN are described in Section 3. Section 4 shows an application of PACDYN in the study of a large AC/DC practical power system. Section 5 shows results obtained in studies of different nature for three other test systems.

Despite the major algorithm and theoretical developments in the field, fully reflected in the computational methods utilized by SSSP [1] and PACDYN packages, there is a pressing need for further research. Section 6 of this paper identifies some of the most fertile grounds for future research and development in this area.

II. OVERVIEW OF METHODS FOR SMALL SIGNAL STABILITY ANALYSIS

The power system electromechanical stability problem can be represented by a set of differential equations together with a set of algebraic equations, to be solved simultaneously with each other:

$$\begin{aligned} \dot{\underline{x}} &= f(\underline{x}, \underline{r}) \\ \underline{0} &= g(\underline{x}, \underline{r}) \end{aligned} \qquad (1)$$

where $\underline{x}$ is the state vector and $\underline{r}$ is a vector of algebraic variables.

Small–signal stability analysis involves the linearization of (1) around a system operating point ($\underline{x}_o$, $\underline{r}_o$):

$$\begin{bmatrix} \Delta\dot{\underline{x}} \\ \underline{0} \end{bmatrix} = \begin{bmatrix} J_1 & J_2 \\ J_3 & J_4 \end{bmatrix} \begin{bmatrix} \Delta\underline{x} \\ \Delta\underline{r} \end{bmatrix} \qquad (2)$$

The power system state matrix can be obtained by eliminating the vector of algebraic variables $\Delta\underline{r}$ in equation (2):

$$\Delta\dot{\underline{x}} = (J_1 - J_2 J_4^{-1} J_3)\,\Delta\underline{x} = \mathbf{A}\ \Delta\underline{x} \qquad (3)$$

The symbol **A** is used to represent the system state matrix, whose eigenvalues provide information on the singular point stability of the non–linear system.

The symbol Δ signifies an incremental change from a steady-state value and will often be omitted in the remaining part of this paper.

II.1 Traditional Algorithms

For many years, programs have been developed to form explicitly the state space equations:

$$\begin{aligned} \dot{\underline{x}} &= A\,\underline{x} + \underline{b}\,u \\ y &= \underline{c}^t\,\underline{x} \end{aligned} \qquad (4)$$

where u and y are a given pair of input and output variables.

Full eigensolution of non–sparse matrix $\mathbf{A}$ is normally restricted to systems of moderate size (≈ 500 states) due to the large memory and computation time requirements.

The transfer function $F(s)$ relating the input u and output y variables is obtained from the Laplace transformation of equation (4):

$$F(s) = \underline{c}^t\,(s\mathbf{I} - \mathbf{A})^{-1}\,\underline{b} \qquad (5)$$

The frequency response analysis of dynamic systems can be performed by replacing the Laplace variable "s" by "$j\omega$" in equation (5) and numerically calculating $F(j\omega)$ for discrete values of "$j\omega$" within the frequency range of interest. The use of equation (5) becomes prohibitive for large order systems due to excessive computational time and memory requirements.

Transfer function residue calculation [10,15], eigenvalue sensitivity coefficients [16], time response to step disturbance and many other needed functions are all prohibitively expensive for large scale systems using this traditional formulation.

II.2 Algorithms for Large Scale Systems

The fundamental concept that allows the methods of the previous section to be applied to large scale systems is the use of the *augmented system equations* [8,11], which is now described.

The basic equation relating state matrix, eigenvalues and eigenvectors is:

$$\mathbf{A}\,\underline{u} = \lambda\,\underline{u} \qquad (6)$$

where λ is a system eigenvalue and $\underline{u}$ its associated eigenvector.

This basic equation when expressed in terms of the Jacobian matrix shown in (2), becomes a generalized eigenvalue problem:

$$\begin{pmatrix} J_1 & J_2 \\ J_3 & J_4 \end{pmatrix} \begin{pmatrix} \underline{u} \\ \underline{r}_u \end{pmatrix} = \lambda \begin{pmatrix} I & 0 \\ 0 & 0 \end{pmatrix} \begin{pmatrix} \underline{u} \\ \underline{r}_u \end{pmatrix} \qquad (7)$$

where $(\underline{u}^t, \underline{r}_u^t)^t$ is the *augmented* right eigenvector of λ and is denoted by $\underline{u}^a$. Similarly, the *augmented* left eigenvector can be defined as $(\underline{v}^t, \underline{r}_v^t)^t$ and is denoted by $\underline{v}^a$.

The state space equations of (4) can in a similar way be expressed as:

$$\begin{pmatrix} \dot{\underline{x}} \\ \underline{0} \end{pmatrix} = \begin{pmatrix} J_1 & J_2 \\ J_3 & J_4 \end{pmatrix} \begin{pmatrix} \underline{x} \\ \underline{r} \end{pmatrix} + \begin{pmatrix} \underline{b}^a \end{pmatrix} u$$

$$y = \begin{pmatrix} \underline{c}_x{}^t & \underline{c}_r{}^t \end{pmatrix} \begin{pmatrix} \underline{x} \\ \underline{r} \end{pmatrix} = \underline{c}^{at}\,\underline{x}^a \qquad (8)$$

where

$\underline{b}^a$ = augmented input vector
$\underline{c}^a$ = augmented output vector
$\underline{x}^a$ = augmented state vector

The large advantage of equations (7) and (8) is that the system Jacobian matrix is highly sparse and allows the use of efficient sparsity–based algorithms. A good part of the algorithms for the solution of small-signal stability problems which make use of the augmented system equations concept are briefly described in this section.

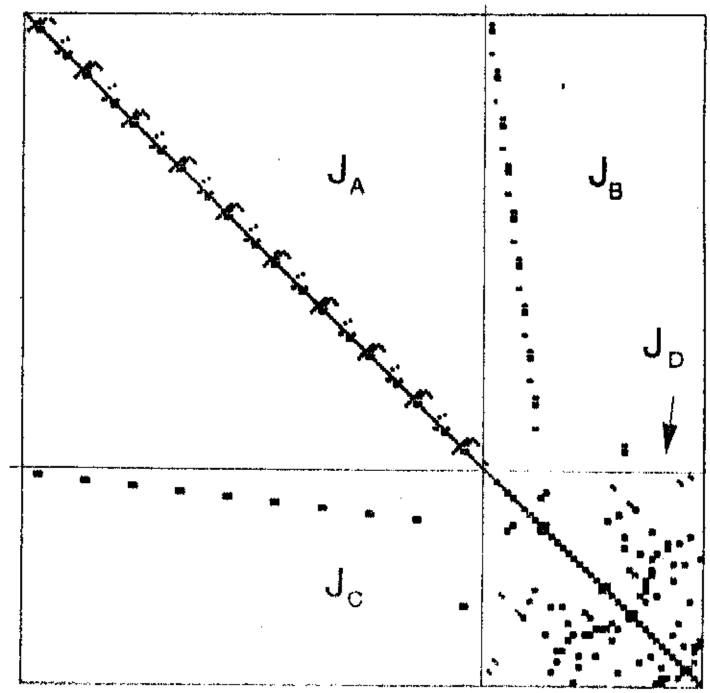

Figure 1. Jacobian Matrix for New England System

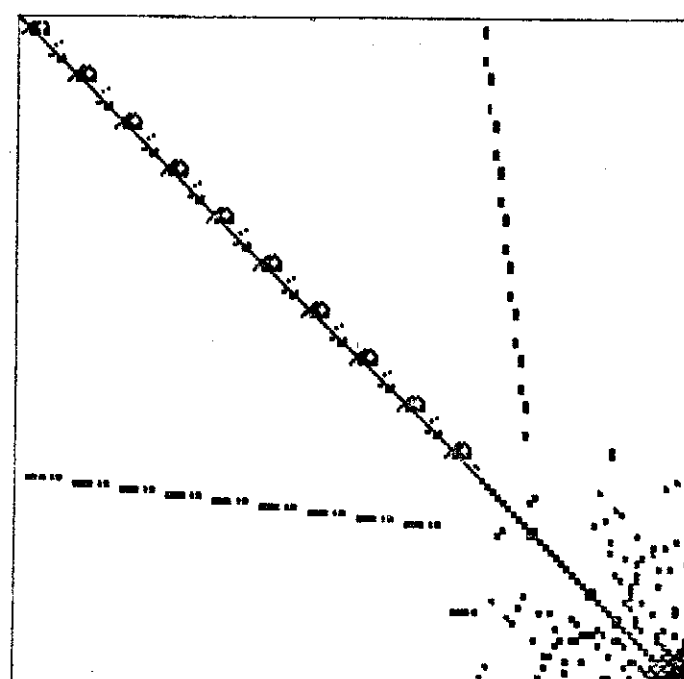

Figure 2. Triangular Factors Topology Map for New England System Jacobian Matrix

Figure 1 shows the Jacobian matrix topology for the well–known New England stability test system [17] where the system variables are ordered in a different way to that shown in equation (2). The reader should refer to [8] for more details on this different assembling of the power system equations.

The Jacobian matrix shown in Figure 1 is real, asymmetric and very sparse. Figure 2 pictures the triangular factors topology map for the Jacobian matrix of this system, which are also highly sparse.

Inverse Iteration

The major computational task in the basic inverse iteration algorithm is related to solving for $\underline{w}_{k+1}$ in the equation below:

$$(\mathbf{A} - q\mathbf{I})\ \underline{w}_{k+1} = \underline{z}_k \tag{9}$$

where the subscript k is the iteration number, q is a complex shift and $\underline{z}_k$ is a complex vector.

Matrix **A** is not sparse for the small–signal electromechanical stability application. Therefore factorizing $(\mathbf{A} - q\mathbf{I})$ and solving for $\underline{w}_{k+1}$ demands a large computational effort if the problem dimension is high.

Computational efficiency is achieved by using sparsity techniques to solve the equivalent matrix problem:

$$\begin{pmatrix} \mathbf{J}_1 - q\mathbf{I} & \mathbf{J}_2 \\ \mathbf{J}_3 & \mathbf{J}_4 \end{pmatrix} \begin{pmatrix} \underline{w}_{k+1} \\ \underline{r}_{k+1} \end{pmatrix} = \begin{pmatrix} \underline{z}_k \\ \underline{0} \end{pmatrix} \tag{10}$$

where $\underline{r}_{k+1}$ is the vector of algebraic variables and $\underline{0}$ is a null vector.

Both right and left *augmented* eigenvectors can be calculated from the same **LU** factors of the asymmetric Jacobian matrix.

Krylov Subspace Methods

Consider $\mathbf{W} = [\ \underline{w}_1\ \underline{w}_2 \ldots \underline{w}_m\ ]$ to be a basis for an invariant subspace of dimension m. Since this is an invariant subspace, the premultiplication **A W** yields a matrix whose columns can be written as linear combinations of the columns of **W** and can be expressed as:

$$\underset{n \times n}{\mathbf{A}}\ \underset{n \times m}{\mathbf{W}} = \underset{n \times m}{\mathbf{W}}\ \underset{m \times m}{\mathbf{C}} \tag{11}$$

The right eigenvalue/eigenvector equation for the coefficient matrix **C** is given by:

$$\mathbf{C}\ \underline{y} = \lambda\ \underline{y} \tag{12}$$

Premultiplying both sides of equation (12) by the matrix **W** and using the relation described in equation (11) one obtains

$$\mathbf{A}\ \mathbf{W}\underline{y} = \lambda\ \mathbf{W}\underline{y} \tag{13}$$

Equation (13) shows that λ is an eigenvalue of both **C** and **A**. In this way the large scale eigenvalue problem (**A**) can be reduced to an equivalent lower order problem (**C**) if an invariant subspace **W** is determined.

This basic concept is utilized in all Krylov subspace methods such as Simultaneous Iteration, Modified Arnoldi and asymmetric Lanczos [18,19].

Frequency Response Calculations

Equation (11) shows an intermediate step in the derivation of equation (5):

$$(\ s\mathbf{I} - \mathbf{A}\ )\ \underline{\mathbf{X}}(s) = \underline{\mathbf{b}}\ \underline{\mathbf{U}}(s) \tag{14}$$

note that $\underline{\mathbf{X}}(s)$ and $\underline{\mathbf{U}}(s)$ are the Laplace transforms of the system state vector and the applied input respectively.

Replacing s by $j\omega$ and noting that (14) is similar to equation (9), the frequency response method can be written as

$$\begin{pmatrix} j\omega\mathbf{I} - \mathbf{J}_1 & -\mathbf{J}_2 \\ -\mathbf{J}_3 & -\mathbf{J}_4 \end{pmatrix} \begin{pmatrix} \underline{\mathbf{X}}(j\omega) \\ \underline{\mathbf{R}}(j\omega) \end{pmatrix} = \begin{pmatrix} \underline{\mathbf{b}} \\ \underline{0} \end{pmatrix} \underline{\mathbf{U}}(j\omega) \tag{15}$$

Normally, generator terminal voltage magnitude and active power are among the output variables of interest. The linearized expressions for these variables in the frequency domain are similar to those in the time domain, and are given by:

$$\Delta V_t(j\omega) = \frac{V_{r0}}{V_{t0}}\ \Delta V_r(j\omega) + \frac{V_{m0}}{V_{t0}}\ \Delta V_m(j\omega) \tag{16}$$

$$P_t(j\omega) = V_{r0}\ \Delta I_r(j\omega) + V_{m0}\ \Delta I_m(j\omega) + I_{r0}\ \Delta V_r(j\omega) + \\ + I_{m0}\ \Delta V_m(j\omega) \tag{17}$$

where the subscript $_0$ denotes a steady-state value for the variable, while r and m stand for real and imaginary components.

The use of expressions of the type shown in (16) and (17) obviates the need to calculate the system output matrix **C**, which is non-sparse, with large savings in computation.

System Equivalents in the Frequency Domain

This methodology is very effective in saving computation time when using the frequency response algorithm of equation (15) [9,20]. In this application it is necessary that the applied disturbance and monitored outputs be all located within the study system. This methodology will be briefly explained through use of Figure 3, where the two generators and associated controllers comprise the study system while the large AC/DC system will be referred to as the external system.

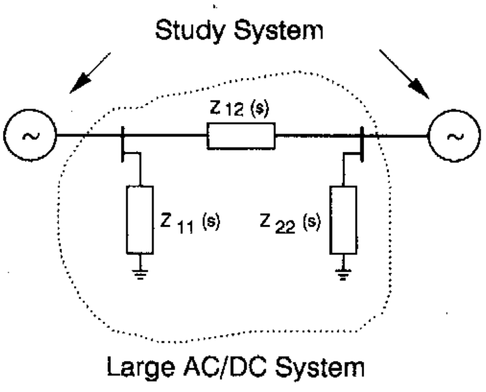

Figure 3. Large System Equivalent in the Laplace Domain

The problem posed is that of studying the dynamic interactions and controller design of the two distinct generators in Figure 3. The operational impedances shown in Figure 3 are described by rational polynomials in s of order equal to the number of state variables in the external system. These high order polynomials are never analytically obtained but rather numerically evaluated for every discrete value of frequency in the range of interest.

A frequency response plot for controller design purposes normally requires from two to three hundred discrete frequency evaluations. Every discrete frequency evaluation involves the factorization and solution of a complex matrix problem, in the form shown in (15), with several thousand equations. The frequency response algorithm is one of the most CPU intensive methods in large scale power system analysis.

The large external system frequency response contributions can be previously calculated and stored on disk files for every discrete value of applied frequency within the range of interest. The interactions within the study system, considering the dynamics of the whole system, can then be calculated from a slightly modified set of equations of the study system that includes the previously calculated external system contributions.

Transfer Function Residues

The transfer function $F(s)$ shown in (5) can be expressed as [10]:

$$F(s) = \underline{c}^t (s\mathbf{I} - \mathbf{A})^{-1} \underline{b} = \sum_{i=1}^{n} \frac{R_i}{s - \lambda_i} \tag{18}$$

where n is the dimension of $\mathbf{A}$ and R_i is the residue of $F(s)$ associated with the eigenvalue λ_i. The residue R_i can be expressed as the product of a mode observability factor ($\tilde{c}_i$) by a mode controllability factor ($\tilde{b}_i$). These two factors can be easily calculated from the knowledge of both right and left augmented eigenvectors and the augmented input and output vectors as described in [10]. Left and right augmented eigenvectors are obtained through use of inverse iteration method shown in (10).

Once the desired right and left eigenvectors are calculated, the residues for thousands of different transfer functions can be efficiently obtained by considering the corresponding augmented input/output vectors.

Eigenvalue Sensitivity Coefficients

The eigenvalue sensitivity coefficients can be calculated, when using matrix $\mathbf{A}$, through the formula

$$\frac{\partial \lambda}{\partial \alpha} = \frac{\underline{v}^t \dfrac{\partial \mathbf{A}}{\partial \alpha} \underline{u}}{\underline{v}^t \underline{u}} \tag{19}$$

where $\underline{u}$ and $\underline{v}$ are the right and left eigenvectors associated with λ and α is a system parameter.

A general formula for eigenvalue sensitivity coefficients applied to the generalized eigenvalue problem was described in [16]. For the *augmented system equations* shown in (7) some simplification applies, yielding:

$$\frac{\partial \lambda}{\partial \alpha} = \frac{\underline{v}_a^t \dfrac{\partial \mathbf{J}}{\partial \alpha} \underline{u}_a}{\underline{v}^t \underline{u}} \tag{20}$$

where $\mathbf{J}$ is the Jacobian matrix shown in (7).

Useful information can be obtained through eigenvalue sensitivity analysis when α is chosen to be a bus voltage magnitude, a network impedance, a dynamic component or controller parameter, etc.

Time Response of the Linearized System

Consider the linearized system state space equations shown in equation (4). A step disturbance is to be applied to the input variable u and the dynamic response of the system monitored through the variables in $\underline{x}$ and y. Adopting the implicit trapezoidal algorithm [21] for the numerical integration of the system equations one obtains:

$$\left(\frac{2}{h}\mathbf{I} - \mathbf{A}\right)\underline{x}_{i+1} = \left(\frac{2}{h}\mathbf{I} + \mathbf{A}\right)\underline{x}_i + 2\,\underline{b} \tag{21}$$

where h is the time step of integration, I the identity matrix and $\underline{x}_i$ and $\underline{x}_{i+1}$ are values at time steps t_i and $t_{i+1} = t_i + h$. By referring to equations (4) and (8) it can be seen that equation (21) is equivalent to:

$$\begin{pmatrix} \frac{2}{h}\mathbf{I}-\mathbf{J}_1 & -\mathbf{J}_2 \\ -\mathbf{J}_3 & -\mathbf{J}_4 \end{pmatrix} \begin{pmatrix} \underline{x}_{i+1} \\ \underline{r}_{i+1} \end{pmatrix} = \begin{pmatrix} \frac{2}{h}\mathbf{I}+\mathbf{J}_1 & \mathbf{J}_2 \\ \mathbf{J}_3 & \mathbf{J}_4 \end{pmatrix} \begin{pmatrix} \underline{x}_i \\ \underline{r}_i \end{pmatrix} + 2\,\underline{b} \tag{22}$$

The algorithm in (22) is efficient when implemented with sparsity coding. Vector $\underline{c}^t$ of equation (4) is not needed since the output variable y can be obtained from simple expressions in terms of the variables contained in the solution vectors $\underline{x}_{i+1}$ and $\underline{r}_{i+1}$.

Transfer Function Zeros

The zeros of the transfer function of equation (5) can be obtained by solving the generalized eigenvalue problem [12]:

$$\begin{pmatrix} \mathbf{A} & \underline{b} \\ \underline{c}^t & 0 \end{pmatrix} \begin{pmatrix} \underline{x} \\ u \end{pmatrix} = \lambda \begin{pmatrix} \mathbf{I} & \underline{0} \\ \underline{0}^t & 0 \end{pmatrix} \begin{pmatrix} \underline{x} \\ u \end{pmatrix} \tag{23}$$

A standard library QZ routine [22] can be used to obtain the complete set of transfer function zeros, as long as the system is of moderate size.

Krylov subspace methods can be used to efficiently calculate several zeros at a time of large power system dynamic models. These methods must be applied to the augmented generalized eigenvalue problem, which is sparse:

$$\begin{pmatrix} \mathbf{J}_1 - q\mathbf{I} & \mathbf{J}_2 & \underline{b}_x \\ \mathbf{J}_3 & \mathbf{J}_4 & \underline{b}_r \\ \underline{c}_x^t & \underline{c}_r^t & 0 \end{pmatrix} \begin{pmatrix} \underline{x} \\ \underline{r} \\ u \end{pmatrix} = \lambda \begin{pmatrix} \mathbf{I} & 0 & \underline{0} \\ 0 & 0 & \underline{0} \\ \underline{0}^t & \underline{0}^t & 0 \end{pmatrix} \begin{pmatrix} \underline{x} \\ \underline{r} \\ u \end{pmatrix} \tag{24}$$

Improved AESOPS

The AESOPS algorithm [17] is a heuristically based one-at-a-time eigenvalue method designed to compute the electromechanical modes of oscillation for large power systems. The AESOPS algorithm is derived from the linearized equation of motion of a chosen generator, to which a complex frequency disturbance in the mechanical torque is applied. At every iteration, a corrected value for this complex frequency disturbance is applied until the system becomes resonant. This iterative process is almost always convergent and the converged complex frequency value corresponds to an electromechanical eigenvalue which is dominant at the disturbed generator.

The power system eigenvalues were shown in [1] to be equal to the zeros of a special transfer function. This fact were not used to advantage in [1] due to the lack of an exact analytical expression for such transfer function and of an adequate transfer function zero finding method for large scale systems. These two obstacles were obviated in the work reported in [12], leading to the improved AESOPS algorithm here described.

Consider the block diagram of Figure 4 which describes the torque-angle loop dynamics of the disturbed j-th generator in a large power system. The inertia constant of the j-th generator is denoted by H_j.

Considering Figure 4 and choosing the mechanical torque and rotor angle as output and input variables respectively, one gets:

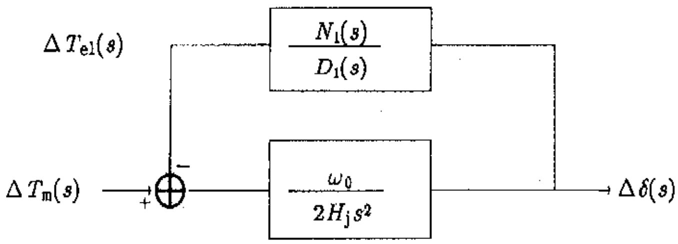

Figure 4. Torque-Angle Loop of Disturbed *j*-th Generator

$$\Delta T_m(s) = \left(\frac{2H_j s^2}{\omega_0} + \frac{N_1(s)}{D_1(s)} \right) \Delta\delta(s) \tag{25}$$

It can readily be seen that the zeros of the transfer function $\Delta T_m(s)/\Delta\delta(s)$ of (25) are equal to the poles of the closed loop system of Figure 4. The desired power system eigenvalues are therefore given by the zeros of the transfer function $\Delta T_m(s)/\Delta\delta(s)$.

The zeros of (25) can be obtained, as shown in [12], by solving the generalized eigenvalue problem:

$$\begin{bmatrix} \mathbf{A'} & \underline{\mathbf{b}}_\delta \\ \underline{\mathbf{c}}^t & d(\lambda) \end{bmatrix} \begin{bmatrix} \underline{\mathbf{x}} \\ \delta \end{bmatrix} = \lambda \begin{bmatrix} \mathbf{I} & \underline{0} \\ \underline{0}^t & 0 \end{bmatrix} \begin{bmatrix} \underline{\mathbf{x}} \\ \delta \end{bmatrix} \tag{26}$$

where the term $d(\lambda)$ is given by:

$$d(\lambda) = c_\delta + \frac{2H_j}{\omega_0}\lambda^2 \tag{27}$$

and c_δ, $\underline{\mathbf{b}}_\delta$ and $\mathbf{A'}$ are defined in [12].

The generalized eigenvalue problem described by equation (10) cannot be adequately solved by the inverse iteration algorithm since the matrix on the left part of the equation is a functional of the unknown variable λ. A more convenient way to solve this problem would be by using the Newton-Raphson method applied to the *augmented system equations* [12].

Mixed Real/Complex Computation

The use of sparse matrix and vector techniques to efficiently solve large simultaneous linear equations is the basis for almost all applications in power systems.

The efficiency of sparsity techniques is dependent on the skillful implementation of the algorithms and the exploitation of the coefficient matrix characteristics like symmetry, blocked structure, etc. Sparse matrix techniques need to be adapted to take full advantage of special characteristics of the matrix problems dealt with in different applications [23].

Power system analysis deals mainly with structurally symmetric matrices, whose elements are either all real or all complex, and very good algorithms have been developed to handle these cases. The existing algorithms are however not fully suited to the different class of matrix problems which arises in the power system small signal stability area.

The power system stability problem is formulated through the *augmented system equations* shown in (4) for the efficient small signal analysis of large scale power systems. The eigenanalysis and frequency domain methods previously described deal with a matrix problem of mixed nature, where a real coefficient matrix (the Jacobian matrix) has complex elements added to just some of its diagonal positions. This fact can be exploited to advantage, resulting in the use of both real and complex arithmetic during the triangular decomposition and repeat solution. A tie–breaker criterion for the minimum–degree ordering [23] is used to minimize the complex arithmetic. A partial refactorization scheme [23] is also readily obtained from the knowledge of the complex pattern of the factors.

These mixed real/complex techniques can be applied to matrix problems in other fields of engineering.

Efficient State Matrix Formation

The state matrix **A** of equation (4) can be directly obtained by performing sparse Gaussian elimination to the Jacobian matrix of (2) [21]. This method is however not efficient for large scale systems due to the inevitable excessive fill–in, since **A** is non-sparse in this application.

An efficient method for obtaining **A** directly from the *augmented system equations* is now described. The large and non-sparse matrix **A** is here formed by calculating one of its columns at a time. Let $\underline{e}_i$ be a singleton [23], i.e., a vector with a real unity value at the *i*–th position and zeros elsewhere. The product $\mathbf{A}\,\underline{e}_i$ yields the *i*–th column of the state matrix **A**. This elementary matrix/vector product constitutes the basis of this algorithm that fully exploits the sparsity of the Jacobian matrix.

Two steps need be performed to obtain $\underline{\mathbf{a}}_i$, the *i*–th column of the state matrix:

1) Solve for vector $\underline{r}_i$

$$\begin{bmatrix} \mathbf{I} & 0 \\ \mathbf{J}_3 & \mathbf{J}_4 \end{bmatrix} \begin{bmatrix} \underline{e}_i \\ \underline{r}_i \end{bmatrix} = \begin{bmatrix} \underline{e}_i \\ \underline{0} \end{bmatrix} \tag{28}$$

2) Perform the product below to obtain $\underline{\mathbf{a}}_i$

$$\begin{bmatrix} \underline{\mathbf{a}}_i \\ \underline{0} \end{bmatrix} = \begin{bmatrix} \mathbf{J}_1 & \mathbf{J}_2 \\ \mathbf{J}_3 & \mathbf{J}_4 \end{bmatrix} \begin{bmatrix} \underline{e}_i \\ \underline{r}_i \end{bmatrix} \tag{29}$$

Note that only one real matrix factorization is needed to obtain all columns of the state matrix **A**.

A modern package for the small–signal analysis of power systems should have a good part of the above described algorithms. A production grade software must have ease of data input, flexible user defined controller models capable of sensing any combination of local and remote system variables and good program output. Program efficiency may be slightly sacrificed in favor of the above facilities.

III. THE PACDYN SOFTWARE PACKAGE

The PACDYN beta version is coded in standard FORTRAN–77 and has been implemented in VAX 11/780, DECstation and IBM–PC compatible (386 or 486) equipment. It presently requires 4 Mb of memory using double precision. This dimension allows the representation of a system with 1000 buses and 1500 lines with complete dynamic data for 200 generators, 10 HVDC links, 30 static VAR compensators and 20 induction motors. Full eigensolution can be obtained for matrices having up to 500 states, using a standard library QR routine [22]. Left and right eigenvectors are obtained through use of inverse iteration applied to the *augmented system equations*.

The operating point condition can also be read from a load flow program history file. All major dynamic components (synchronous and induction machines, automatic excitation systems, speed governors, stabilizing signals, static VAR compensators, HVDC links, advanced series capacitors and static phase-shifters) can be modeled in various degrees of detail.

PACDYN has user–defined controller subroutines which allow complete freedom in defining the order and topology of the various controllers in the system. Any combination of local and remote variables may be used as input to any given controller (up to 20 different inputs per controller).

All the algorithms are directly implemented using the very sparse power system Jacobian matrix of equation (2), which is the kernel of the package. This structured implementation has some major advantages: 1) any new development or addition to the Jacobian matrix is automatically valid to all implemented algorithms; 2) a single set of specially designed sparsity routines [13] yield efficient solutions for all algorithms alike.

A number of new features and functions are under current development:

- multiterminal HVDC systems;
- advanced series compensator and static phase shifter models;
- inclusion of network RLC transients and adequate component models for SSR studies [24];
- voltage stability analysis capability (please refer to paper section Concluding Remarks);
- eigenvalue sensitivity with respect to system changes;
- graphical interface;
- parallel computer implementation of Krylov subspace methods.

Unique Features

The PACDYN package has some unique features that distinguish it from other small–signal stability analysis packages:

1) The time response algorithm, that allows a wide variety of input disturbances and the efficient monitoring of any specified set of system variables. This is a highly useful complementary function for the analysis and control of small–signal stability of large dynamic systems. It allows a direct validation with the traditional transient stability simulation results.

2) The use of system equivalents in the frequency domain allows large savings in controller design through frequency response techniques considering the whole power system dynamics.

3) User defined controller routines that allow the representation of system controllers of any kind, order and topology. A maximum of 20 different input variables per controller may be used and selected from a wide variety of system variables either local or remote. These routines are used for the modeling of controllers such as AVR, speed governors, PSS, SVC, HVDC links and FACTS devices.

4) All functions are available in a single computer program. Different program functions can be run in a highly interactive mode using the same system Jacobian matrix. As a single data file and program is used, the possibility of user generated input errors is largely minimized. Code maintenance also highly benefits from this program characteristic.

5) Fast determination of ranking lists, based on transfer function residues, for stabilizing control allocation to damp a specified mode of oscillation.

6) Calculation of zeros of scalar and matrix transfer functions;

7) Mixed real/complex sparse factorization and solution routines for computational speed–up.

IV. BRAZILIAN SOUTH–SOUTHEAST HVDC INTERCONNECTED SYSTEM RESULTS

The power system analyzed is the South–Southeast Interconnected Brazilian system for a heavy load condition of the year 1993. The system model has 122 generators, 1800 buses, 2600 lines and one HVDC link. Sixty six generators and associated controllers are modeled in detail while the remaining are represented as negative impedances.

Figure 5 shows the schematic diagram of the AC/DC Itaipu Transmission System which delivers 12,600 MVA to the South and Southeast Systems.

For the purposes of this analysis all loads were modeled as constant impedances and the stabilizing signal of Itaipu 60 Hz excitation was assumed disconnected.

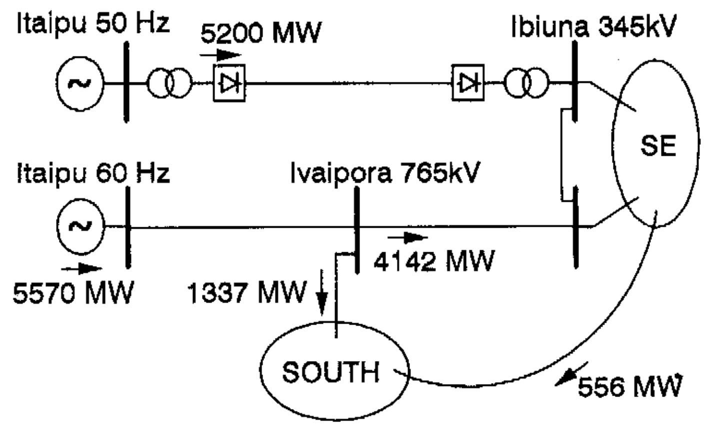

Figure 5. Schematic Diagram of Itaipu AC/DC Transmission System

Effect of HVDC Link Dynamics on Major System Oscillatory Mode

In order to determine the influence of the HVDC link dynamics in a major system oscillatory mode, for the particular system operating point, two cases were investigated: 1) no HVDC dynamic modeling (negative impedance representation at Ibiuna bus); 2) HVDC link model comprising converter equations, DC line time constant, constant current control at the rectifier and minimum area criterion for the inverter firing control.

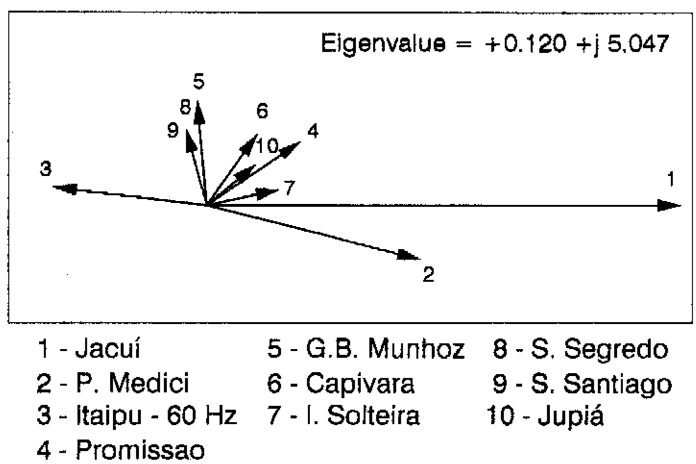

Figure 6. Rotor Speed Mode–Shape ($\lambda = +0.120 \pm j\,5.047$)

In both cases the system model showed an unstable oscillatory mode between Itaipu and the South and Southeast System. The critical eigenvalues were $\lambda = +0.120 \pm j\,5.047$ for case 1 and $\lambda = +0.117 \pm j\,5.010$ for case 2. Figure 6 shows a phasor diagram containing the participation of some generators in the rotor speed mode–shape for the first case. The mode–shape for the second case is practically identical to the first. One can therefore conclude that the dynamic HVDC model has a small effect on this 0.8 Hz unstable mode in the absence of HVDC link modulation, for the operating point investigated.

Stabilization of Brazilian System Model through HVDC Link Modulation

The stabilizing signal design of any dynamic component in the system can be obtained through frequency response techniques. The reader is referred to [11] for a detailed description on this subject.

Figure 7 shows a block diagram which describes the complete system dynamics through the HVDC link rectifier control loop. This block diagram is similar to the ones used in [11] for the design of stabilizing signals to generator excitation systems and static VAr compensators.

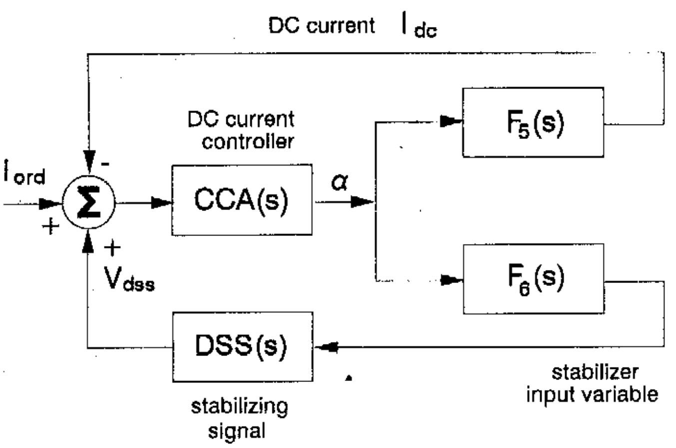

Figure 7. Power System Representation Through the HVDC Rectifier Control Loop

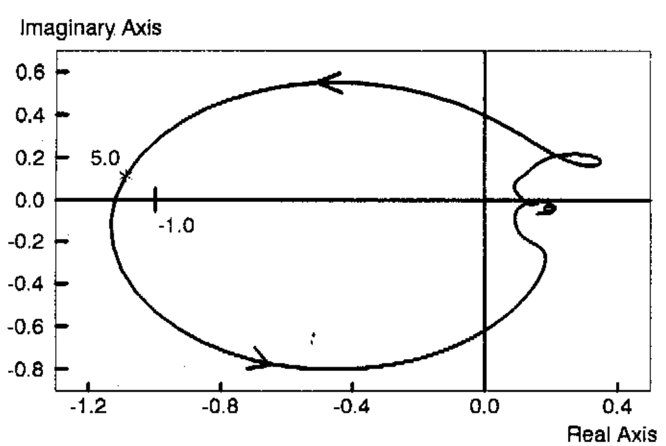

Figure 8. Nyquist Plot of $\Delta P_t(s)$ / $\Delta I_{ord}(s)$

A Nyquist diagram was obtained for the transfer function $\Delta P_t(s)$ / $\Delta I_{ord}(s)$ (see Figure 8) where $\Delta P_t(s)$ denotes electrical power deviations of Itaipu 60 Hz generator. The analysis of this diagram shows there is no need for phase compensation in the stabilizing signal and that the minimum direct gain in the stabilizer feedback loop required for system stabilization would be around one. With such gain, the Nyquist plot for the open–loop transfer function $\Delta V_{dss}(s)$ / $\Delta I_{ord}(s)$ is exactly like Figure 8 and just encloses the –1 point in the desired counter–clockwise direction.

The critical eigenvalue has a good damping for a stabilizer gain $k_{dss} = 10$ ($\lambda = -0.29 \pm j\,4.75$), which gives a gain margin slightly above 10 according to the Nyquist plot of Figure 8.

The HVDC control stabilizer transfer function DSS(s) comprises a washout block with reset constant of 3 seconds and a direct gain equal to 10. Note that the washout block is only needed to ensure a zero stabilizer output in steady–state.

Time responses of this linearized system are presented in figures 9 and 10 for a 1% step disturbance applied to the reference voltage of the Itaipu 60 Hz excitation system. The monitored variables are voltage magnitude deviations at the buses Ibiuna, Ivaipora and Itaipu. Figure 9 shows the Brazilian Interconnected System response, without the Itaipu 60 Hz stabilizer, where the 0.8 Hz unstable oscillations are quite evident.

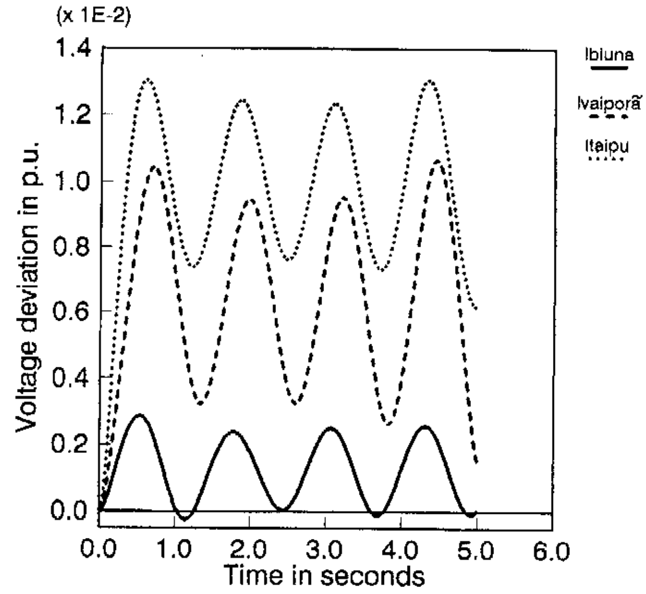

Figure 9. Unstable System Time Response ($\lambda = +0.117 \pm j\,5.010$)

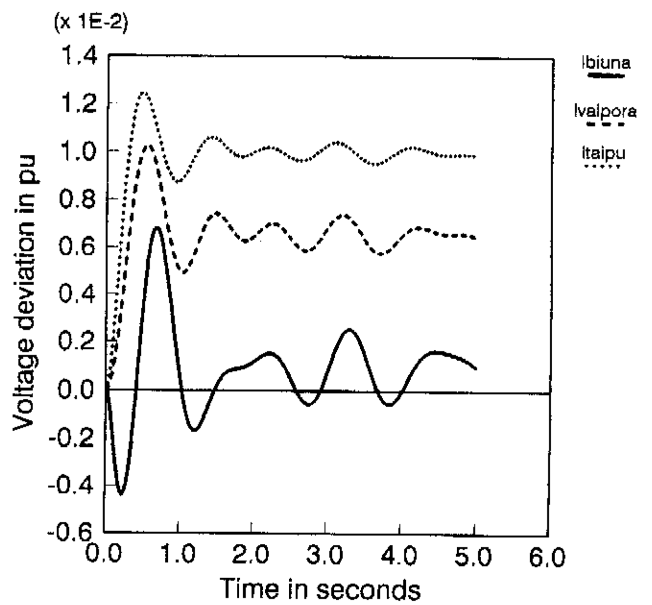

Figure 10. Stable System Time Response ($\lambda = -0.29 \pm j\,4.75$)

Figure 10 shows the system response after stabilization achieved through the use of the previously designed HVDC link stabilizing signal.

Controller design is normally carried out through linear techniques. Controller dynamic performance following large disturbances should be verified by non–linear time response simulations.

Effect of Transmission Voltage Level on Oscillation Damping

The study system here is practically the same as that of the previous section. The major differences are: 1) the system loads characteristics, which are now of the constant current (MW) and constant impedance (MVAr) types; 2) the Itaipu 60 Hz generator has its PSS properly included; 3) the Itaipu Transmission System is now slightly overloaded.

Figure 11 shows the critical eigenvalue location for three different voltage profiles of the Itaipu 765 kV AC transmission system. The results showed the damping of the critical oscillatory mode to be very sensitive to the Itaipu transmission voltage level. A low voltage profile along the 765 kV system may even lead to oscillatory mode instability. These results clearly reinforce the need to adopt a high voltage profile strategy in the operation of the 765 kV Itaipu Transmission System.

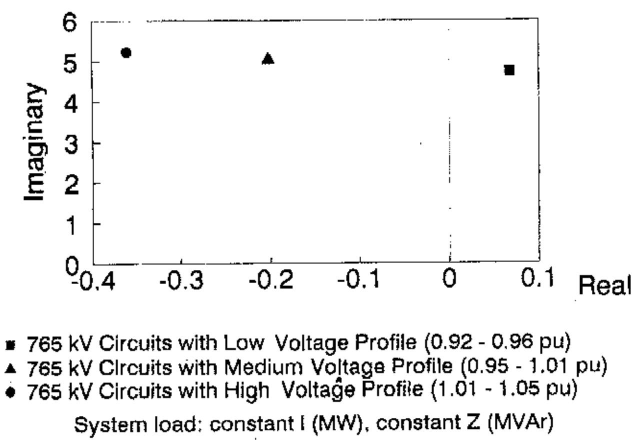

Figure 11. Critical Eigenvalue Location for Different Voltage Levels

V. OTHER PACDYN RESULTS

Three other examples are given to illustrate the use of PACDYN in the solution of different practical problems.

Centralized Control Strategy for Multiple Static VAr Compensators in Long Distance Voltage Supported Transmission Systems

The results of this section are taken from [25], which reports succesfull results on the coordinated control of multiple SVC's in a long distance voltage supported transmission system. Figure 12 shows the basic configuration of the transmission system analyzed in [25].

The system contains a 9600 MVA power plant connected to an infinite bus through three 765 kV circuits with total transmission lenght of 1600 km.

The generation dispatch considered yielded an operating point with a large angular displacement (175°) between the generator field and the infinite bus voltage.

Reference [25] analises different SVC control strategies of local and centralized nature. Control structure C of [25] has every SVC with an individual controller modeled according to Figure 13, having five input signals, apart from two reference voltage signals. This SVC controller corresponds to a centralized voltage control strategy (ΣV_i) incorporating a secondary local voltage control loop, with integral action and slower time constant. The stabilizing signal to this SVC controller is also derived from the sum of the terminal bus frequencies ($\Sigma\dot{\theta}$) of the various SVC's (see Figure 14). Note that every remote bus voltage or frequency channel in Figures 13 and 14 has a single time lag of 50 ms to model the telecommunication delay.

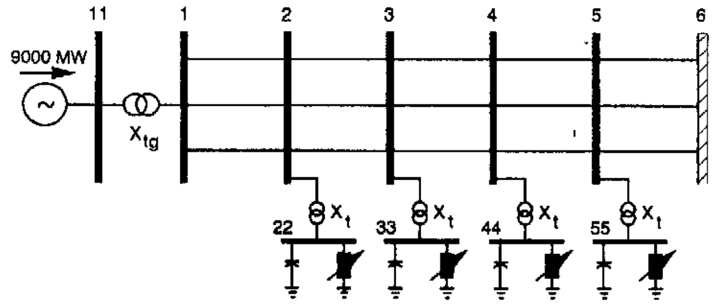

Figure 12. Voltage Supported AC Transmission System

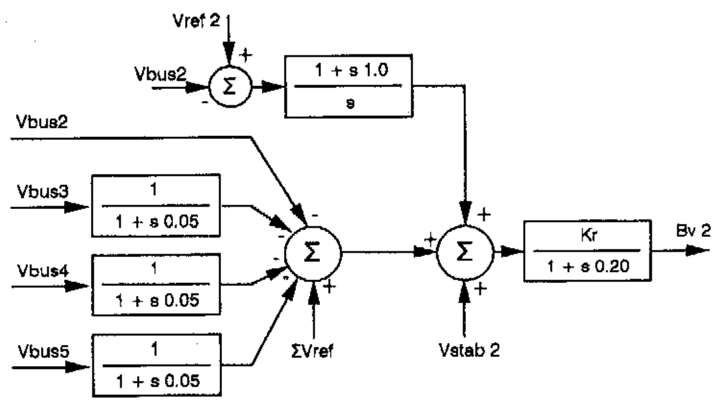

Figure 13. Control Structure C – Centralized Voltage Control Strategy with a Secondary Local Voltage Control Loop (this diagram is for the SVC at bus 22)

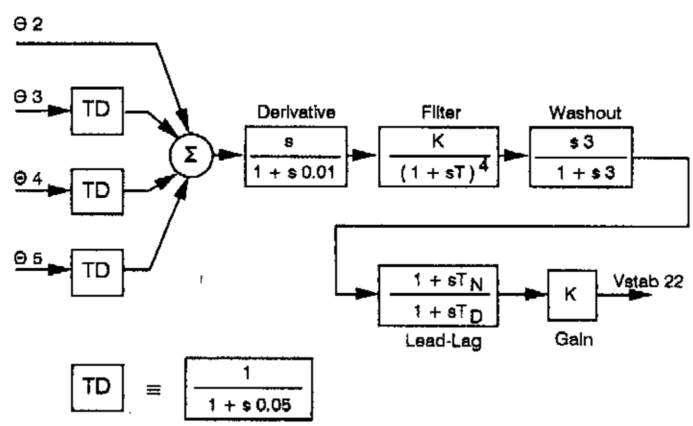

Figure 14. Stabilizer Structure for Centralized Damping Control (this diagram is for the SVC at bus 22)

The centralized control strategy proposed in [25] is conceptually simple, but leads to controllers with a large number of feedback signals. The user-defined controller routines of PACDYN allow easy data preparation of controller structures even more complex than those of Figures 13 and 14.

The results obtained showed that the centralized strategy for voltage and oscillation damping control is more robust [26] than the traditional control which is based on local measurements. This can be observed from the time response plots of Figures 15 and 16 which correspond to a line outage condition between buses 1 and 2 of the transmission system. Figure 15 shows the system dynamic performance when having a traditional control scheme where every SVC and its stabilizer sense only local variables. Figure 16, on the other hand, corresponds to the centralized control structure depicted in Figures 13 and 14. Both control structures had been tuned for an adequate performance considering a base case power flow. It is quite evident that the centralized control structure ensures an adequate dynamic performance for the line-outage condition while the traditional control can not avoid system instability.

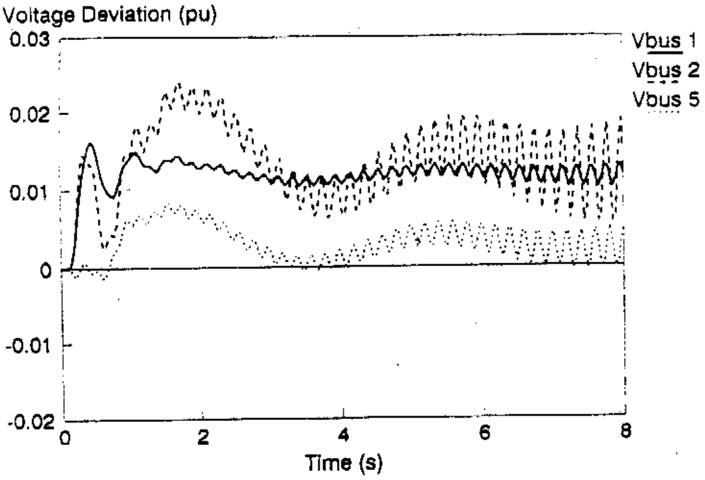

Figure 15. Control Structure A with Local Frequency Stabilizer

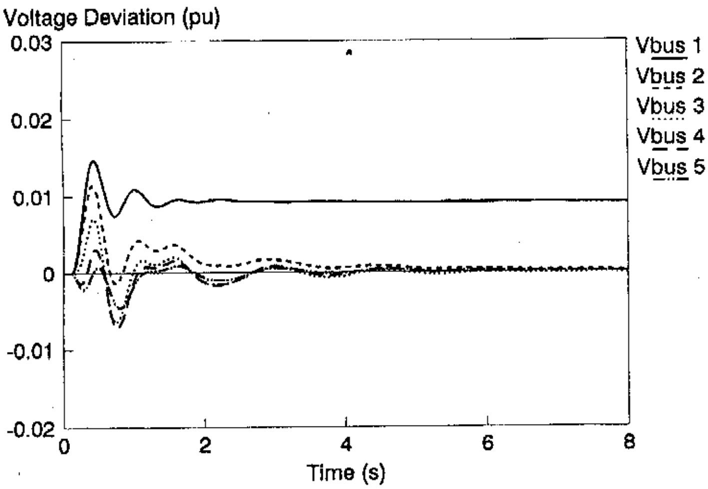

Figure 16. Control Structure C with $\Sigma\Theta_i$ Stabilizer

SVC Location for Damping Oscillations

The location of a SVC is determined taking into account various factors, such as static and dynamic voltage support, capability of damping electromechanical oscillations, etc. The algorithm implemented in PACDYN is intended to find the best SVC location for the sole purpose of damping electromechanical oscillations. The algorithm is based on transfer function residues and can determine the location of a SVC for a given operating condition for power systems of any topology [10].

The two-area system chosen to be studied here is almost identical to that of [27] except for the generator and excitation control parameters which were not available. The transmission circuit was divided into ten sections of equal lenght yielding the eleven-bus network shown in Figure 17. Various power flow conditions were considered and residues associated with the inter-area mode of oscillation calculated for all transfer functions $\Delta V_i(s)/\Delta B_i(s)$, $i = 1,...,nb$. The symbols ΔV_i and ΔB_i denote incremental changes in voltage magnitude and shunt admittance at the *i*-th system bus respectively. Integer *nb* denotes the total number of buses in the system. The tridimensional surface of Figure 18 shows the variation of the moduli of these residues as function of both power transfer level and SVC location. It is seen that the residues have larger magnitude for buses near the middle of the transmission circuit and that they increase with the power transfer. When there is no power interchange between areas the residues are comparatively very low and at the mid-point of the transmission circuit (bus 6) the residue is equal to zero. Therefore, for this operating condition, the inter-area mode of oscillation is not observable nor controllable from the mid-point of the transmission circuit.

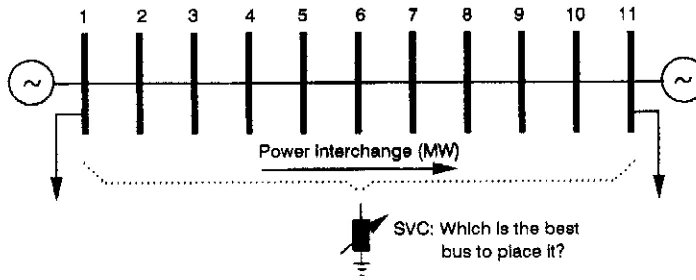

Figure 17. Two-area test system

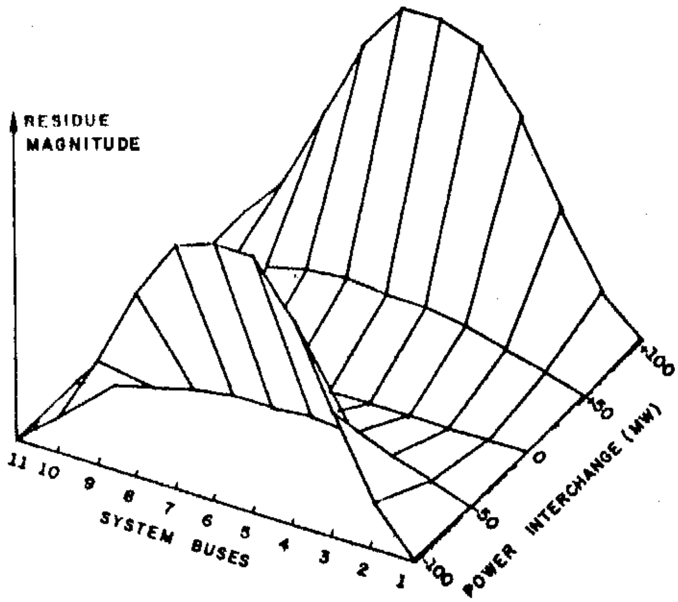

Figure 18. Residue Magnitude as a Function of Power Interchange and Network Location

These results are in accordance with [27] showing that the SVC should be located near the mid-point of the transmission circuit and that it becomes more effective in damping the inter-area mode of oscillation for higher power transfer levels.

Zeros of Scalar and Matrix Transfer Functions

The knowledge on the location of transfer function zeros enables control engineers to carry out controller design more effectively. There has recently been some increased interest in zeros in association with the power system damping control problem [10,11,12,28,29,30]. The PACDYN algorithms for the efficient calculation of zeros in large scale power system models were presented in [12]. This reference also contains results on scalar and matrix transfer function zeros for a five-machine power system and discusses their effect on the system stabilization. A summary of these results are presented in this section.

The 5-machine system is shown in Figure 19 and full data is provided in [11]. The machines are referred to as G_1, G_2, G_3, G_4 and G_7 according to the buses where they are connected. Machine G_7 is a dynamic equivalent for a power-importing area which is represented as a large synchronous motor.

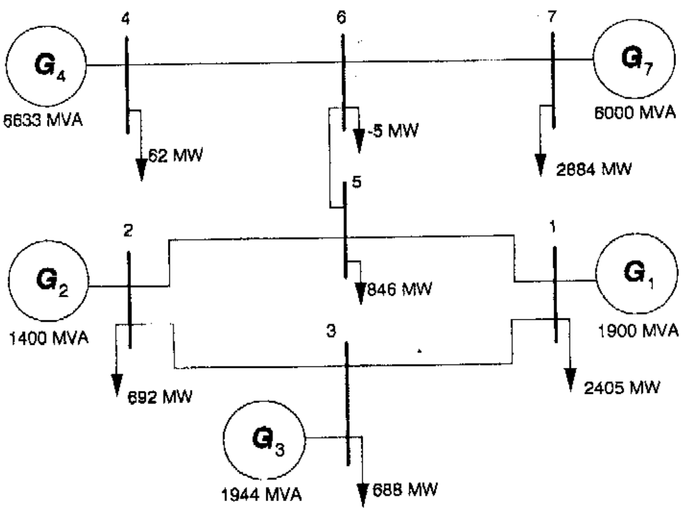

Figure 19. 5-Machine System

This system has a pair of unstable eigenvalues $\lambda = +0.646 + j\,5.391$ and any attempt to stabilize it through excitation control on G_4 is bound to fail. Figure 20 shows the root locus of the critical eigenvalues as the gain of a rotor speed-derived stabilizer at the G_4 generator is varied. The critical electromechanical mode is seen to always remain unstable due to the presence of an unstable pair of zeros in the $\Delta w^4(s)/\Delta V_r^4(s)$ transfer function ($z = +0.049 + j\,5.908$).

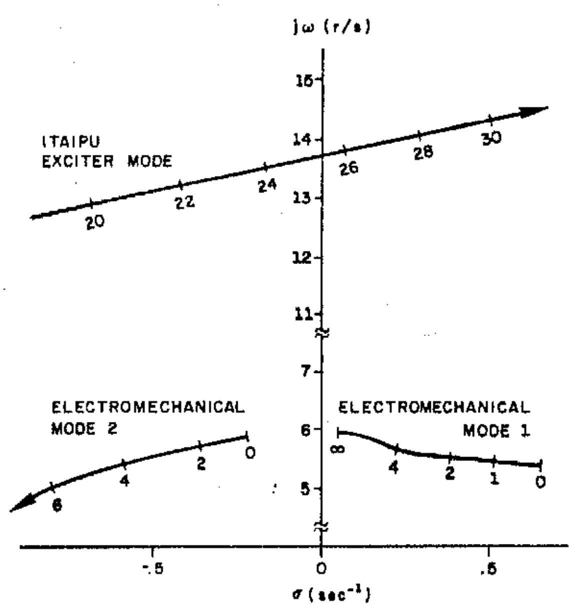

Figure 20. Root Locus as a Function of the Gain of the Stabilizer at the G_4 Generator

The ability to calculate matrix transfer function zeros, or transmission zeros, is useful in determining a minimum set of generators for placing stabilizers and effectivelly damp unstable oscillations. Transmission zero results are shown here for the 5-machine system.

The transfer function matrix shown below relates the reference voltages, $\Delta V_r^i(s)$, of generators G_1, G_2 and G_3 to their rotor speed deviations $\Delta\omega^i(s)$:

$$\begin{matrix}\Delta V_r^1(s)\\ \Delta V_r^2(s)\\ \Delta V_r^3(s)\end{matrix} \longrightarrow \begin{bmatrix} g_{11}(s) & g_{12}(s) & g_{13}(s)\\ g_{21}(s) & g_{22}(s) & g_{23}(s)\\ g_{31}(s) & g_{32}(s) & g_{33}(s)\end{bmatrix} \longrightarrow \begin{matrix}\Delta w^1(s)\\ \Delta w^2(s)\\ \Delta w^3(s)\end{matrix}$$

This matrix has a transmission zero $z = +0.61 + j\,5.34$, which is very close to the unstable system pole $\lambda = +0.646 + j\,5.391$. The multivariable root locus for this multi-input-multi-output system, as the stabilizer gains at generators G_1, G_2 and G_3 are varied will have a root locus branch between this unstable pole-zero pair, irrespective of the stabilizer transfer functions. This clearly shows that the unstable mode is uncontrollable from these three generators.

On the other hand, the transfer function matrix:

$$\begin{matrix}\Delta V_r^1(s)\\ \Delta V_r^4(s)\end{matrix} \longrightarrow \begin{bmatrix} g_{11}(s) & g_{12}(s)\\ g_{21}(s) & g_{22}(s)\end{bmatrix} \longrightarrow \begin{matrix}\Delta w^1(s)\\ \Delta w^4(s)\end{matrix}$$

has well damped transmission zeros, the least damped being $z = -1.839 + j\,9.157$ and $z = -1.273 + j\,6.635$. This indicates that the system can be made stable by adding stabilizers to generators G_1 and G_4, provided their parameters are properly chosen.

VI. CONCLUDING REMARKS

Despite the major algorithmic and theoretical developments, there is a pressing need for further research. This section comments on some of the topics which deserve special attention.

A few decades ago the stability assessment of a characteristic polynomial was carried out through use of the Routh–Hurwitz criterion. Despite its limitations, it was used in practice. Other root finding techniques were neither numerically robust nor efficient for high order systems. With the advent of modern computers, the use of state variable concept and the powerful QR eigenvalue routines, stability assessment was made possible for systems of much larger order. Present day limitations stand between order 500 to 800 for a complete eigensolution of asymmetric **A**, on a uniprocessor computer. Full eigensolutions have recently been reported for power system models with 2200 state variables using a super computer [31].

Considering the case of the large scale dynamic systems, a massive amount of computation and large CPU time is still needed to answer two apparently simple questions: 1) is the system stable? 2) which are the least damped eigenvalues?

The same problem, which existed a few decades ago, remains: there is a need for a fast stability assessment method for large scale dynamic systems. The S–matrix method, described in [19], was an attempt in this direction. Despite the claims of their originators, neither the authors of this paper nor Ontario Hydro specialists [1] could however obtain satisfactory results with the use of the S–matrix method.

There is intensive research activity in the development of eigenvalue methods for use in parallel computers [32]. These developments have already extended the application of numerically stable QR method to state matrices of larger size. Further developments could eventually provide an answer to the present need for a fast stability assessment tool.

There is no established methodology for the simultaneous design of multiple controllers in large electrical power systems. The conventional single–machine–infinite–bus equivalent has worked well when tuning generator excitation control stabilizers (PSS) in large systems [33]. The PSS's in a multimachine environment usually show robust performance and low dynamic interaction. This is not the case with SVC's or any other FACTS devices, all of which have a high speed of response.

In a multiple FACTS environment, there may be a high dynamic interaction between these devices and their tuning must therefore be done in a more coordinated manner [25,34]. Multi-variable frequency response techniques may provide a partial solution to this problem. Multiple pole location techniques also show interesting possibilities [35].

The possibility of fast partial eigensolution through use of parallel computers may open the possibility of implementing this function in future Energy Management Systems. One can envision an even more appealing piece of software as a long–term research development: a security–constrained redispatch with post-contingency corrective actions which ensures adequate damping of system oscillations [35].

A recent development has given PACDYN the capability for voltage stability analysis. The modal analysis methodology of [36] has been implemented with additional improvements. Once the critical eigenvalues associated with the voltage collapse have been calculated, valuable information on corrective measures can be obtained through transfer function residues. Residues can be used to determine the critical branches and loads. The best generators for voltage control and the best locations for additional voltage support can also be determined.

The phenomena of fast voltage collapse (several seconds time frame) have a high interaction with the dynamics of the various power system components and controllers: generators, excitation systems, static VAr compensators, HVDC links, etc [37,38,39,40,41]. The adequate simulation of these phenomena is a highly complex task since results are very sensitive to the modeling of the load dynamics. PACDYN represents a valuable tool for the analysis of these problems.

We conclude by stressing the high benefits of having a comprehensive linear analysis package for the study of small-signal electromechanical and voltage stability problems. A good package should allow the study of large power systems, having a wide variety of components and controller structures, in a CAE environment, where various linear control methods can be used in a complementary manner.

ACKNOWLEDGEMENTS

The authors are grateful to Mr. Marcio Szetchman, Research and Development Director of CEPEL, for having provided strategic support to this project in Brazil and abroad. The continuous support and encouragement from Mr. Edmundo A.P. da Silva, manager of System Analysis Division, of the System Operation Department of FURNAS Centrais Elétricas S.A., greatfully acknowledged.

REFERENCES

[1] **P. Kundur, G.J. Rogers, D.Y. Wong, L. Wang & M.G. Lauby**, "A Comprehensive Computer Program Package for Small Signal Stability Analysis of Power Systems", *IEEE Trans. on Power Systems*, **PWRS–5**, pp.1076–1083, 1990

[2] **CIGRÉ**, "Questionaire on Electromechanical Oscillations Damping in Power System – Report on the Answers", *Electra*, **no.64**, pp.59–70, 1979

[3] **Brazilian Operations Planning Coordinating Council**, *Study of Machine Controllers Tuning for Dynamic Performance Improvement of the North–Northeast Brazilian Interconnected System*, Report SCEL–GTAS, no. 26/89, September 1989 (in Portuguese)

[4] **Brazilian Operations Planning Coordinating Council**, *Parameter Optimization of Controllers of the Major Power Stations of the South–Southeast Brazilian Interconnected System*, Report SCEL–GTAS/S, no. 07/90, May 1990 (in Portuguese)

[5] **Brazilian Operations Planning Coordinating Council**, *Analysis of the Recorded Spontaneous Oscillations During Light Load Condition on the South–Southeast Brazilian Interconnected System*, Report SCEL–GTPO, no. 12/91, 1991 (in Portuguese)

[6] **P. Gomes, A.L.B. Bonfim, A. Pedroso & N. Martins**, "Application of Eigenvalue Techniques in Power System Dynamics", *Proceedings of 1st Symposium of Electric Operation and Expansion Planning*, Rio de Janeiro, August 1987

[7] **N. Martins & R. Baitelli**, *User's Guide to Program AUTOVAL V.4.0*, CEPEL, October 1987 (in Portuguese)

[8] **N. Martins**, "Efficient Eigenvalue and Frequency Response Methods Applied to Power System Small-Signal Stability Studies", *IEEE Trans. on Power Systems*, Vol. **PWRS-1**, pp. 217-226, February 1986

[9] **N. Martins & L.T.G. Lima**, "Decomposition Technique for Efficient Computation of Small–Signal Stability Problems in Large Power Systems", *Proc. of IASTED Conference on High Technology in the Power Industry*, pp. 232–237, Scottsdale, Arizona, March 1988.

[10] **N. Martins & L.T.G. Lima**, "Determination of Suitable Locations for Power System Stabilizers and Static VAr Compensators for Damping Electromechanical Oscillations in Large Scale Power Systems", *IEEE Trans. on Power Systems*, Vol. **PWRS–5**, pp.1455–1469, November 1990

[11] **N. Martins & L.T.G. Lima**, "Eigenvalue and Frequency Domain Analysis of Small–Signal Electromechanical Stability Problems", *IEEE Symposium on Application of Eigenanalysis and Frequency Domain Methods for System Dynamic Performance*, publication **90TH0292–3PWR**, pp. 17–33, 1990

[12] **N.Martins, H.J.C.P.Pinto and L.T.G.Lima**, "Efficient Methods for Finding Transfer Function Zeros of Power Systems", *Proceedings of 1991 IEEE Power Industry Computer Application Conference*, pp. 320–328, May 1991

[13] **L.T.G. Lima, N. Martins & H.J.C.P. Pinto**, "Mixed Real/Complex Factorization", in *1992 IEEE/PES Winter Meeting*, paper **92 WM 288–1 PWRS**, New York, Jan.1992

[14] **N.J.P. Macedo, N. Martins, H.J.C.P. Pinto & L.T.G. Lima**, "Application of a Modern Computational Package in the Small–Signal Stability Analysis of the Brazilian System", *Proceedings of IV CIGRÉ/ERLAC Conference*, Puerto Iguazu, Argentine, August 1991 (in Portuguese)

[15] **V. Arcidiacono, E. Ferrari, R. Marconato, J. Dos Ghali e D. Grandez**, "Evaluation and Improvement of Electro-mechanical Oscillation Damping by Means of Eigenvalue-Eigenvector Analysis. Practical Results in the Central Peru Power System", *IEEE Trans. on Power Apparatus and Systems*, Vol. **PAS–99**, pp.769–778, March/April 1980

[16] **T. Smed**, "Feasible Eigenvalue Sensitivity for Large Power Systems", presented at *1992 IEEE/PES Winter Meeting*, paper **92 WM 171–9 PWRS**, New York, January 1992

[17] **R.T. Byerly, D.E. Sherman & R.J. Bennon**, "Frequency Domain Analysis of Low–Frequency Oscillations in Large Electric Power Systems", *EPRI EL–726 Project RP 744–1 Final Report, Part 1*, Palo Alto, CA, April 1982

[18] **L. Wang & A. Semlyen**, "Application of Sparse Eigenvalue Techniques to the Small Signal Stability Analysis of Large Power Systems", *IEEE Trans. on Power Systems,* Vol. **PWRS-5**, pp.635–642, 1990

[19] **N. Uchida & T. Nagao**, "A New Eigen–Analysis Method of Steady-State Stability Studies for Large Power Systems: S Matrix Method". *IEEE Trans. on Power Systems*, Vol. PWRS–3, pp. 706–714, May 1988.

[20] **H.Suzuki & others**, "Midterm Stability Analysis of a Multimachine System by the Frequency Response Method", *Electrical Power and Energy Systems*, Vol. 1, no.1, pp.16-20, April 1979

[21] **H.W. Dommel & N. Sato**, "Fast Transient Stability Solutions", *IEEE Trans. on PAS*, Vol. **PAS–91**, pp.1643-1650, July/August 1972

[22] **B.T. Smith, J.M. Boyle, J. Dongarra, B. Garbow, Y. Ikebe, V.C. Klene & C.B. Moler**, *Matrix Eigensystem Routines: EISPACK Guide*, 2nd Edition, Springer–Verlag, New York, 1976

[23] **Alvarado, F.L., Tinney, W.F. and Enns, M.K.**, "Sparsity in Large-Scale Network Computation", to appear in *Advances in Electric Power and Energy Conversion System Dynamics and Control,* Academic Press, C.T.Leondes ed., 1991

[24] **P.M. Anderson, B.L. Agrawal & J.E. Van Ness**, *Subsynchronous Resonance in Power Systems*, IEEE Press, New York, 1990

[25] **N. Martins, N.J.P. Macedo, L.T.G. Lima & H.J.C.P. Pinto**, "Control Strategies for Multiple Static VAR Compensators in Long Distance Voltage Supported Transmission Systems", *paper submitted to 1992 IEEE/PES Summer Meeting*

[26] **J.R. Smith**, "A Perspective on Robust Multivariable Control of Large Power Systems", in *Proc. of EPRI/NSF Workshop on Application of Advanced Mathematics to Power Systems*, Redwood City, CA, September 1991

[27] **H.V. Larsen, J.H. Chow**, "SVC Control Design Concepts for System Dynamic Performance", in *IEEE Tutorial Course: Application of SVS for System Dynamic Performance*, publication **87 THO 187 5 PWR**, pp. 36–53, 1987

[28] **J.F. Hauer**, "Reactive Power Control as a Means of Enhanced Interarea Damping in the Western U.S. Power System – A Frequency-Domain Perspective Considering Robustness Needs", in *IEEE Tutorial Course: Application of SVS for System Dynamic Performance*, publication **87 THO 187–5 PWR**, pp. 79–82, 1987

[29] **A.M.A. Hamdan & A.M. Elabdalla**, "Stability Assessment of Multimachine Power Systems Using Multivariable Frequency Response Methods", *Electric Power System Research*, Vol. **12**, pp. 209–218, 1987.

[30] **M. Klein, G.J. Rogers, S. Moorty, P. Kundur**, "Analytical Investigation of Factors Influencing Power System Stabilizers Performance", *1992 IEEE/PES Winter Meeting*, paper **92 WM 016–6 EC**, New York, January 1992.

[31] **J.F. Hauer & D.M. Elwood**, "BPA Runs MASS on Cray Supercomputer to Support SVC Additions", *EPRI Newsletter*, August 1991

[32] **R.Schreiber**, "Short Bibliography in Parallel Matrix Computation", *Proceedings of EPRI/NSF Workshop on Application of Advanced Mathematics to Power Systems*, Redwood City, CA, September 1991

[33] **P. Kundur, M. Klein, G.J. Rogers & M.S. Zywno**, "Application of Power System Stabilizers for Enhancement of Overall System Stability", *IEEE Trans.on Power Systems*, Vol.4, no.2, pp.614–626, May 1989

[34] **N.G. Hingorani**, "FACTS – Flexible AC Transmission System", *Proceedings of EPRI Workshop The Future in High Voltage Transmission: Flexible AC Transmission System (FACTS)*, Cincinnati, Ohio, November 1990

[35] **N.Martins**, "Some Present and Future Activities in CEPEL's Power System Dynamics Area", *Proceedings of EPRI/NSF Workshop on Application of Advanced Mathematics to Power Systems*, San Francisco, September 1991

[36] **B. Gao, G.K. Morrison & P. Kundur**, "Voltage Stability Evaluation Using Modal Analysis", *1991 IEEE/PES Summer Meeting*, San Diego, July 1991

[37] **Th. Van Cutsem**, "Dynamic and Static Aspects Of Voltage Collapse", *Proceedings of Bulk Power System Voltage Phenomena – Voltage Stability and Security*, **EPRI EL-6183**, pp. 6.5 – 6.79, January 1989

[38] **C.W. Taylor,** "Concepts of Undervoltage Load Shedding for Voltage Stability", *1991 IEEE/PES Winter Meeting*, paper 91 **WM 162-8 PWRD**, New York, February 1991

[39] **CIGRE TF 38-01-03**, "Planning Against Voltage Collapse", *Electra*, No. 111, March 1987

[40] **L.A.S. Pilloto, M. Szechtman, and A.E. Hammad**, "Transient AC Voltage Related Phenomena for HVDC Schemes Connected to Weak AC Systems", *1991 IEEE/PES Summer Meeting*, paper **91 SM 305-3 PWRD**, July 1991

[41] **A. Hammad, M. El-Sadek**, "Prevention of Transient Voltage Instabilities due to Induction Motor Loads by Static VAr Compensators", *IEEE Transactions on Power Systems*, **Vol. 4, No. 3**, pp 1182-1188, August 1989

Nelson Martins (M'1981, SM'1991) received his B.Sc. degree from the University of Brasilia, Brazil, in 1972. He received the M.Sc. and Ph.D. degrees, both in electrical engineering, from the University of Manchester, UK, in 1974 and 1978 respectively.

Dr. Martins is presently a senior research engineer at CEPEL, the Brazilian electrical energy research center located in Rio de Janeiro. He works in the development of methods and computer tools for power system dynamics and control.

Leonardo T.G. Lima received his B.Sc. and M.Sc. degrees, both in electrical engineering, from Federal University of Rio de Janeiro, Brazil, in 1986 and 1991 respectively.

Mr.Lima worked in CEPEL until 1988 and presently is a lecturer at the Department of Electrical Engineering, Instituto Militar de Engenharia, Rio de Janeiro, Brazil. His current work and interests include power system dynamics and development of large scale power system analysis tools.

Herminio J.C.P.Pinto received his B.Sc. and M.Sc. degrees, both in electrical engineering, from the Federal University of Rio de Janeiro, Brazil, in 1986 and 1990 respectively. Since 1986 he is with CEPEL and his current work and interests include power system operation and control and parallel processing.

Nilo J.P. Macedo received his B.Sc. degree in Electrical Eng. in the Catholic University in Rio de Janeiro in 1979.

Mr. Macedo is a senior engineer at Furnas Eletricity Co., where he works in power system operations planning.